Ultra-distal tephra deposits and Bayesian modelling constrain a variable marine radiocarbon offset in Placentia Bay, Newfoundland

Alistair J. Monteath[1], Matthew S. M. Bolton[2], Jordan Harvey[2], Marit-Solveig Seidenkrantz[3], Christof Pearce[3], Britta Jensen[2]

[1]Geography and Environmental Science, University of Southampton, Southampton, SO17 1BJ, UK
[2]Earth and Atmospheric Sciences, University of Alberta, Edmonton, T6G 2E3, Canada
[3]Department of Geoscience, Arctic Research Centre, and iClimate, Aarhus University, Aarhus, DK-8000, Denmark

Correspondence to: Alistair J. Monteath (a.j.monteath@soton.ac.uk) or Matthew Bolton (bolton1@ualberta.ca)

Abstract. Radiocarbon dating marine sediments is complicated by the strongly heterogeneous age of ocean waters. Tephrochronology provides a ~~well-established~~well-established method to constrain the age of local radiocarbon reservoirs and more accurately calibrate dates. Numerous ultra-distal cryptotephra deposits (non-visible volcanic ash >3000 km from source) have been identified in peatlands and lake sediments across north-eastern North America~~,~~ and correlated with volcanic arcs in the Pacific north-west. Previously, however, these isochrons have ~~never~~ not been identified in sediments from the north-west Atlantic Ocean. In this study, we report the presence of two ultra-distal cryptotephra deposits; Mazama Ash and White River Ash eastern lobe (WRAe), in Placentia Bay, North Atlantic Ocean. We use these well dated isochrons to constrain the local marine radiocarbon reservoir offset (ΔR) and develop a robust Bayesian age-depth model with a ΔR that varies through time. Our results indicate that the marine radiocarbon offset in Placentia Bay was -126±151 years (relative to the Marine20 calbration curve) at the time of Mazama Ash deposition (7576~~62~~2±18 yr BP~~C.E.~~) and -396±144 years at the time of WRAe deposition (1098~~852~~ -1097~~853~~ yr BP~~C.E.~~). Changes in ΔR appear to coincide with inferred shifts in relative influences of the inner Labrador Current and the Slopewater ~~c~~Current in the bay. An important conclusion is that single-offset models of ΔR are easiest to apply and often hard to disprove. However, such models may oversimplify reservoir effects in a core, even over relatively short time scales. Acknowledging potentially varying offsets is critical when ocean circulation and ventilation characteristics have differed over time. The addition of tephra isochrons permits the calculation of semi-independent reservoir corrections and verification of the single ΔR model.

1 Introduction

Tephrochronology (the "*identification, correlation and dating of tephra layers*"; Thorarinsson, 1981; Lowe and Hunt, 2001) is an age-equivalent technique that can be used to date or synchronise, palaeoenvironmental and archaeological records over a range of timescales and distances (Lowe, 2011). This method is particularly valuable in establishing chronologies for marine sediment records that are inevitably depleted in radiocarbon relative to the atmosphere. The depletion in radiocarbon is mainly a result of long oceanic residence times and is called the marine reservoir age (R) (Reimer and Reimer, 2001). Due

to large stocks of "old carbon" in ocean waters, organisms that incorporate marine carbon (e.g. foraminifera, fish, marine mammals, molluscs, etc.) typically have a radiocarbon age that appears older than terrestrial organisms of an equivalent age (Ascough et al., 2005). Therefore, a correction must be applied to accurately calibrate radiocarbon dates from ocean sediments (Heaton et al., 2020). Selecting an appropriate correction, however, is not straightforward as the radiocarbon age of ocean water bodies is strongly heterogeneous and may not have remained consistent through time (Gordon and Harkness, 1992; Reimer and Reimer, 2001; Alves et al., 2018). For example, during the Holocene, the global average marine reservoir age varies between 700-350 years (Heaton et al., 2023). Deviations from the average marine reservoir age are expressed as the local marine radiocarbon reservoir offset (ΔR). Tephrochronology provides an independent means to partially address these issues and establish local marine radiocarbon offsets (e.g., Pearce et al., 2017). These data can also reveal past changes in ocean circulation. For example, a comparison between age-depth models established from radiocarbon-dated marine macrofossils (e.g., molluscs and foraminifera) and tephrochronology showed that local marine radiocarbon offsets on the north Icelandic Shelf varied by up to 450 years as the influence of radiocarbon-depleted, Arctic water masses fluctuated (Knudsen and Eiríksson, 2002; Eiríksson et al., 2004, 2011).

Since the identification of ultra-distal cryptotephra deposits in Nordan's Pond Bog, Newfoundland (Pyne-O'Donnell et al., 2012) (Fig. 1), a series of studies have investigated peatlands and lake deposits, throughout the eastern seaboard of north-eastern North America, for the presence of volcanic ash (e.g. Jensen et al., 2014; Pyne-O'Donnell et al., 2016; Mackay et al., 2016, 2022; Spano et al., 2017; Monteath et al., 2019). This research has identified >30 well defined cryptotephra deposits (Jensen et al., 2021), some of which extend into the North Atlantic region (Zdanowicz et al., 1999; Jennings et al., 2014) and as far as western Europe (Jensen et al., 2014; Plunket and Pilcher, 2018). These tephra deposits are derived from a range of eruption sizes (e.g., Mazama Ash ~176 km^3 erupted volume, Buckland et al., 2020; South Mono 0.171-0.195 km^3 erupted volume, Bursik et al., 2014), where long-range deposition was likely influenced by some combination of eruption size, style, duration, and atmospheric conditions/circulation (e.g., the jet stream; Bursik et al. 2009). While large explosive eruptions may be expected to affect greater areas, in general, understanding what is controlling the exceptional dispersal of some tephra deposits and not others is still not well resolved (Pyne-O'Donnell et al., 2012; Jensen et al., 2021).

The Holocene cryptotephra record is uniquely well dated, through a network of chronometers and age models, including layer counting in ice cores (Sigl et al., 2016, 2022; Toohey and Sigl, 2017). There has, however, been no successful attempt to extend eastern North America's tephrostratigraphic framework to ocean cores in the north-western North Atlantic Ocean. Resolving chronological ambiguity in palaeoceanographic records from this region would be particularly valuable as it includes the confluence of the Labrador Current and the North Atlantic Current – both of which are influential components of the sub-polar gyre and Atlantic Meridional Overturning Circulation (AMOC) (Fig. 1). In this study, we identify ultra-distal, North American cryptotephra deposits in marine gravity core AI07-10G from Placentia Bay at the western seaboard of the North Atlantic Ocean (Fig. 1). We go on to use these isochrons to constrain the local marine radiocarbon reservoir offset and develop a robust Bayesian age-depth model. Finally, we highlight the potential for further studies of North American, ultra-distal cryptotephra deposits in ocean sediments while considering some of the remaining challenges.

1.1 Placentia Bay, North Atlantic Ocean

Placentia Bay is located immediately south of Newfoundland, Canada, on the north-western margin of the North Atlantic Ocean. The bay is bordered by the Avalon Peninsula to the east, the Burin Peninsula to the west and the Isthmus of Avalon to the North (Fig. 1). To the south, the seaward opening of the bay is approximately 100 km wide. Water depths exceed 400 m in the bay, which is around 130 km long. Placentia Bay is typically free from sea ice year round, although ice can form between mid-February and late April during the coldest winters. Iceberg sightings in the bay are rare. Between C.E. 1974-2003 sightings only occurred in seven years (30 sightings total) (Catto et al., 1999; Mello and Rose, 2005). The hydrology of the bay is strongly influenced by the inner branch of the Labrador Current, with lesser input from the Slopewater Current, a minor bifurcation from the Gulf Stream (Catto et al., 1999) (Fig. 1). The cold, inner Labrador Current flows south from Baffin Bay as a surface current and includes substantial outflow from Hudson Strait (Drinkwater, 1996). In contrast, the Slopewater current branches north from the Gulf Stream and brings warm, saline waters from the sub-tropics, at subsurface depths, towards southern Newfoundland.

During the Last Glacial Maximum (~Marine Isotope Stage 2), Placentia Bay was glaciated by the Laurentide ice sheet; as a result, drumlins, moraines and megascale lineations are present across the sea floor (Shaw et al., 2006, 2013). The bay was deglaciated prior to the Younger Dryas climate reversal (12,800-11,600 cal yr BP; Pearce et al., 2013; Mangerud, 2021), although the precise timing of ice retreat is not well constrained (Dyke et al., 2002; Shaw et al., 2006, 2013). The varying sea floor topography has resulted in heterogeneous deposition rates, and differing basal ages are reported from sediment cores across the bay, which allows for the development of palaeo-records with various temporal lengths and resolutions. The potential for differing temporal records and sensitivity to elements of both the Labrador Current and Gulf Stream make Placentia Bay an ideal natural laboratory for studying past ocean/atmosphere interactions. As a result, numerous studies have developed palaeo-environmental records from the bay, all of which rely on radiocarbon chronology, necessitating the adoption of marine reservoir corrections (e.g., Jessen et al., 2011; Solignac et al., 2011; Pearce et al., 2014; Sheldon et al., 2016).

2 Methods and materials

2.1 Core AI07-10G

Core AI07-10G measure~~d~~ 460 cm in length and was drilled~~taken~~ in 2007 from 231.3 m water depth at 47.2389°N, 54.6140°W, in Placentia Bay, North Atlantic Ocean. Sheldon et al. (2016) presented the results from radiocarbon dating (Table 1), Itrax-XRF core scanning, and benthic foraminiferal assemblage analyses. These results were combined with analyses from two other cores in Placentia Bay (12G and 14G; Sheldon et al. 2016) to form a composite full Holocene record.

2.2 Tephra extraction and analysis

To quantify volcanic glass shard concentrations in core AI07-10G (reported as shards per gram of dried sediment), we processed continuous 5-cm wide samples taken throughout the sequence, with no gaps between samples, to identify sediment intervals where cryptotephra deposits might be found (ranger finder counts). We subsequently analysed the 5-cm intervals where higher abundances of tephra grains were identified at 1-cm intervals to pinpoint the position of cryptotephra deposits (Pilcher and Hall, 1992).

We extracted glass shards from the host ~~material~~ sediment by drying samples at 105 °C overnight before immersing ~~the material~~sediment samples in 10 % hydrochloric acid and sieving them at 80 µm and 25 µm. Larger size fractions (>80 µm) were retained; however, given the low shard concentrations in core AI07-10G (<40 shards per gram) were not investigated further (Abbott et al., 2018a). Following this, we used stepped, heavy liquid (sodium polytungstate) floatation at 2.00 g/cm^3 and 2.50 g/cm^3 to concentrate volcanic glass, which was mounted on slides and counted under a high-power microscope (Turney et al., 1998).

As no basaltic glass (which is denser than rhyolitic glass) was observed in the initial counts, we extracted glass shards for electron probe microanalysis (EPMA) by sieving samples at 20 µm, followed by heavy liquid floatation at 2.15 g/cm^3 and 2.45 g/cm^3. The extracted material was then mounted in epoxy resin within acrylic stubs and polished to expose the internal glass surfaces before carbon coating (Lowe et al., 2011).

The chemical compositions of individual glass shards (one analysis each) from samples taken at 195-190 cm and 35-30 cm were determined by EPMA, with wavelength dispersive spectrometry on a JEOL 8900 Superprobe at the University of Alberta. A suite of 10 elements (Si, Ti, Al, Fe, Mn, Mg, Ca, Na, K, Cl) were measured using a 5 µm beam diameter with a 15 keV accelerating voltage, and 6 nA beam current, with time-dependent intensity corrections applied to Na to compensate for the ~~smaller~~ narrow beam (<10 µm) diameter (e.g., Jensen et al., 2008, 2021). In addition, we ran two secondary standards of known compositions alongside samples from Placentia Bay to check for instrumental drift and analytical precision: i) Lipari rhyolitic obsidian ID3506 and ii) Old Crow tephra (Kuehn et al., 2011). The major-minor element compositions of glass shards are presented as normalised weight percent (wt %) oxides in comparative diagrams. The complete dataset and associated standard measurements are reported in the supplementary information (Tables S1, S2).

2.3 Bayesian age-depth modelling

To incorporate chronological information from the ultra-distal cryptotephra isochrons identified in core AI07-10G, we developed two different Bayesian age-depth models using OxCal v 4.4.4 (Bronk Ramsey 2009). The ~~full~~ complete code for both models is available in the supplementary information (supplementary text 1.1).

Model I is conceptually the same as the age-depth models described by Sheldon et al. (2016). In this model, radiocarbon dates (Table 1) were calibrated with the Marine20 curve (Heaton et al., 2020) with a single reservoir correction applied to the whole core (-29±45 yrs). In this case, we have ~~informative~~ preliminary information regarding the most probable reservoir

correction range based on ~~near-modern~~ radiocarbon dating of near-modern marine organisms. In Bayesian statistics, this data is called a prior, e.g., a representation of the state of knowledge regarding a parameter, expressed as a probability distribution, before considering all available information (e.g., stratigraphic context). For Model I, we used a prior distribution for the reservoir correction of the weighted mean of the 20 nearest points from Reimer and Reimer's (2001) marine reservoir correction database (Table S3), updated for use with Marine20 (-29±45 yrs). The core top was also included as an age constraint. We assume an exponential prior at zero depth, from 2007.7 CE (the approximate date of collection) decaying to 1000 years earlier with a time constant (τ) of 50 yrs. The deposition was modelled as a Poisson process (i.e., a *P_Sequence*; Bronk Ramsey, 2008) with a nominal number of depositional events (k_0) of 1 per cm. The *k* parameter was permitted to vary within a wide range (i.e., two orders of magnitude on either side of k_0) and was selected through Markov chain Monte Carlo (MCMC) iterations (Bronk Ramsey and Lee, 2013). These settings are the default for sequences with a depth scale in centimetres.

Model II is similar to Model I; radiocarbon dates are calibrated with the Marine20 curve, the same core top constraint is applied, and the model is formulated as a *P_Sequence* using the same parameters. However, Model II differs from Model I in two ways: (1) it includes cryptotephra deposits to constrain the chronology further, and (2) the model calculates multiple ΔR values - varying the radiocarbon reservoir offset throughout the sequence. We used ~~the~~ Mazama Ash (7572±18 yr BP; Sigl et al., 2016, 2022) and White River Ash eastern lobe (WRAe) (1097±1 C.E.; Toohey and Sigl, 2017) as age constraints, both of which are geochemically verified in core AI07-10G (see 3.1 Tephrostratigraphy). Shard counts from both cryptotephra deposits consist of low concentrations and do not have a clearly defined, sharp peak (Fig. 2). These variable and broader peaks are likely caused by downward translocation of shards through sediment loading or bioturbation (Griggs et al., 2015), and complicate the precise stratigraphic depth of the isochrons. In order to incorporate this uncertainty into the Bayesian models we took a conservative approach and used age uncertainties associated with the 5-cm ranger finder counts, rather than the 1-cm point finder counts. To do this, we first estimated the sediment deposition rate from model I at the central depth of both tephra samples. Then, we propagated the depth uncertainty to the tephra age by adding uniform noise in the time dimension. The prior for each cryptotephra deposit was modelled using ages derived from ice core layer counting (a normal distribution; Sigl et al., 2016, 2022; Toohey and Sigl, 2017) plus chronologic sampling uncertainty (u), where u = sampling resolution/deposition rate.

Model II also differed from Model I and earlier approaches (Solignac et al., 2011; Sheldon et al., 2016) by including multiple independent ΔR estimates (i.e., each radiocarbon date had its own ΔR estimate). Each ΔR value was defined (as above) by a mean correction of -29, however, the uncertainty was expanded to ±224 years (i.e., 4x the uncertainty from Reimer and Reimer's 2001 database). This conservative uncertainty regime was adopted to permit the ~~MCMC~~Markov chain Monte Carlo (MCMC) approach inherent to OxCal's sequence modelling to generate an appropriate (non-truncated) posterior estimate for the corrections. A normal -29±224 prior was assumed for all radiocarbon dates except one. For the upper-most radiocarbon date (AAR-15764), we provided an even more forgiving prior (a uniform distribution centred at zero and spanning 2000 years). This prior was selected because the WRAe mean depth is only 2 cm above this sample (Fig. 2). The MCMC is kept

flexible by giving a wide uniform prior. Therefore, the tephra age can strongly inform the ΔR for this date, providing a clearer picture of the necessary reservoir effect around WRAe time.

3 Results and discussion

3.1 Tephrostratigraphy

Using multiple lines of evidence, Wwe identified two discreet discrete cryptotephra deposits in core AI07-10G (Fig. 2) that can be robustly correlated with volcanic eruptions in North America using multiple lines of evidence. Evidence includes stratigraphic order, shard morphology and glass major-minor elements (wt%), which were interrogated using both bi-plots, Log-ratio transformationcompositional Principle Component Analysis (PCA) (Filzmoser et al., 2009; Templ et al., 2011; Vera, 2020) and similarity coefficients (supplementary text 2) (Borchardt et al., 1972). In both cases, the glass EPMA data were consistent and did not include glass shards with different chemical compositions or signs of weathering that might indicate reworking (Abbott et al., 2018a).

3.1.1 Cryptotephra deposit 10G_195 (Mazama Ash)

Cryptotephra deposit 10G_195 was identified between 195-190 cm depth (192.5 cm depth peak) and is formed of colourless, platy and fluted shards, with rhyolitic chemical compositions (Fig. 2). Shard morphology, stratigraphy and glass major-minor elements (similarity coefficient 0.95) are all consistent with Mazama Ash (Fig. 3), which has been identified in study sites throughout north-eastern North America (Pyne-O'Donnell et al., 2012; Spano et al., 2017; Jensen et al., 2021). The Mazama Ash was derived from a VEI 7 (Volcanic Explosive Index) eruption of Mount Mazama (Crater Lake), Oregon, that was amongst the largest volcanic eruptions to take place during the Holocene with an estimated erupted volume of ~176 km^3 (Buckland et al., 2020). Visible ash layers from this event extend throughout much of western North America (Jensen et al., 2019), and cryptotephra deposits are reported in the Greenland ice cores and, potentially, Western Europe (Zdanowicz et al., 1999; Plunket and Piltcher, 2018). Mazama Ash has been precisely dated to 7572±18 yr BP by ice core layer counting (Zdanowicz et al., 1999; Sigl et al., 2016, 2022) and 7682–7584 cal. yr BP by Bayesian age modelling, including from 81 radiocarbon dates (Egan et al., 2015).

3.1.2 Cryptotephra deposit 10G_35 (White River Ash eastern lobe)

Cryptotephra deposit 10G_35 was identified between 35-30 cm depth (32.5 cm depth peak) and is composed of colourless, highly vesicular or pumiceous shards with rhyolitic chemical compositions (Fig. 2). Shard morphology, stratigraphy and glass major-minor elements (similarity coefficient 0.95) are all consistent with White River Ash eastern lobe (WRAe) (Fig. 3), which has been identified in study sites throughout north-eastern North America (Pyne-O'Donnell et al., 2012; Mackay et al., 2016, 2022; Monteath et al., 2019; Jensen et al., 2021). The WRAe is derived from a magnitude 6.7 (VEI 6; erupted volume 39.4-61.9 km^3) Plinian eruption of Mt. Churchill, Alaska (Lerbekmo, 2008; Mackay et al., 2022), and extends

eastward from the Wrangell Volcanic Field. Ash from this eruption has been identified in the Greenland ice cores and numerous study sites from western Europe, where it was first described as the AD860 cryptotephra (Coulter et al., 2012; Jensen et al., 2014). The WRAe has been precisely dated by ice core layer counting, which constrains the eruption timing to the winter of ~~852/853~~1097±1 yr BP~~C.E.~~ (Toohey and Sigl, 2017) – consistent with proximal stratigraphy and Bayesian age modelling (using 28 radiocarbon dates) that dates the eruption to 1175-1075 cal yr BP (West and Donaldson, 2000; Davies et al., 2016).

3.2 Bayesian age-depth modelling

The presence of Mazama Ash and WRAe allows ~~for~~ the Placentia Bay marine reservoir offset to be assessed at multiple points during the Holocene. Results from Model II, which includes the cryptotephra isochrons, show that around Mazama Ash the radiocarbon offset was moderately more negative (i.e., -126±151 relative to the prior ΔR of -29±45 years) (Fig. 4). The large uncertainty range (relative to the offset) associated with ~~the~~ Mazama Ash is caused by our conservative modelling approach that uses the 5 cm range finder results to place the isochron, and the slow accumulation rate at this point in the core (~0.05 cm yr^{-1}). Around WRAe, the radiocarbon offset was larger~~;, e.g.,~~ -396±144 (Fig. 4). Around the ages of both tephra deposits, ΔR values must be more negative than previously assumed to account for the tephra ages. That is, modelled ages are made to be older than would be suggested by the original prior~~, t.~~ Therefore generally, less old carbon is contributing to the system at the study site than modelled for the global ocean. The ΔR varies ~~considerably~~ throughout the age-depth model and particularly around the WRAe isochron. At this depth, there is a large shift in ΔR near WRAe. We modelled a posterior offset of -451±151 years for radiocarbon date AAR-15764, but only -10±213 years for radiocarbon date AAR-17060, 42 cm lower in the core. ~~Therefore, although t~~The reservoir age for both periods of tephra deposition was lower than indicated by Reimer and Reimer's (2001) marine reservoir correction database~~, h~~. However,~~, it was substantially lower~~this offset appears larger in the Early Holocene than in the Mid Holocene. This ~~large~~ apparent difference in ΔR may be explained by either artefacts in the chronology (e.g., radiocarbon date AAR-15764 is inaccurate) or real variance in the age of water bodies. However, as discussed below, the two tephra isochrons were deposited during periods characterised by different hydrographical conditions, and the difference in ΔR for the two tephra deposits likely reflects real differences in the radiocarbon age of the water bodies affecting the site.

Across the whole core, there is an average ΔR difference between the two models of 74 years, but as high as 416 yrs at 34.5 cm, not far below the WRAe, and 126 (a secondary maximum) directly at the mean Mazama depth. In most places, ~~these~~ changes in the more flexible Model II ~~changes~~ do not represent a departure beyond the two-sigma age range of Model I. Indeed, the only portion of the core that does exceed this range and precludes the implicit null hypothesis (no change) is near the WRAe (31.8-35.7 cm) (Fig. 4). Both cryptotephra isochrons push the Bayesian model towards older values (Fig 4.). It is possible that this is caused by inaccurate placing of the position of the cryptotephra isochrons and that Model I is correct. For this to be the case, then both cryptotephra isochrons would be expected to occur deeper in the core (e.g., WRAe would have had to occur at 39.3 cm depth – almost 5 cm below the observed peak at 35-30 cm depth; Fig. 2) and the observed peak in

shard abundance would need to have been reworked upwards into the overlying sediments. Upward movement of the cryptotephra deposits to an extent where the position of the isochron is misplaced seems unlikely, however, as in both cases shard counts are considerably higher at the denoted isochron depth (which already includes 5 cm uncertainty) than below.

Considering the marked departure of ΔR around the time of the precisely dated WRAe from the near-modern prior, we observe that radiocarbon reservoir effects can shift rapidly because of environmental and systemic changes (e.g., carbon source and ocean circulation shifts) over time. Further, the reservoir correction uncertainty may be more substantial in marine settings than suggested by near-modern samples. We conclude that conventional means of relaying proxy records over time often fail to account for time uncertainty. A natural remedy to this failure, and one we advocate for palaeoenvironmental proxy studies, is to propagate the age-uncertainty of an age model ensemble to proxy records (e.g., McKay et al., 2021).

3.3 The implications, potential and challenges of using ultra-distal tephra isochrons in ocean-sediments

3.3.1 Implications and potential applications

Comparative tephrochronological and radiocarbon-dated age models have provided good evidence for past changes in water masses (Knudsen and Eiríksson, 2002; Eiríksson et al., 2004, 2011) and we revised the AI07-10G core chronology with similar aims to improving understanding of regional ocean circulation. Sheldon et al. (2016) used Itrax-XRF core scanning~~,~~ and benthic foraminiferal assemblage analyses to suggest that the influx of the warm Slopewater Current ~~dominated the area~~was more dominant in Placentia Bay during ~~in~~ the Early-Mid Holocene, when ~~the~~ Mazama Ash (~~7622~~7572±18 yr BP~~C.E.~~) was deposited. After ca. 7300 cal yr BP, the inner Labrador Current strengthened, weakening the inflow of the warmer Slopewaters. Even though the inner Labrador Current weakened again in the Late Holocene (after ca. 4000 cal yr BP), during which the WRAe Ash (1098-1097 yr BP~~852-853 C.E.~~) was deposited, the influence of the Slopewater Current did not become as pronounced as in the Early Holocene. Therefore, the difference in ΔR seen at ~~the~~ Mazama Ash compared with the WRAe Ash may reflect actual differences in the radiocarbon age of the water masses affecting Placentia Bay. It also suggests ~~stronger ventilation, and therefore younger reservoir age, of~~ the inner Labrador Current, which includes a substantial terrestrial component from Hudson Strait, has a younger reservoir age ~~Slopewater~~ compared with the waters from the ~~Labrador~~ Slopewater Current.

Identification of Mazama Ash and WRAe in ocean sediments from the north-western North Atlantic highlights the potential for using ultra-distal cryptotephra deposits to constrain marine radiocarbon offsets in this region. More than thirty unique glass populations have been identified in north-eastern North America (Jensen et al., 2021), many of which are correlated with eruptions with well-constrained (decadal or even annual) age ranges. Several of these provide opportunities to synchronise marine records for differing ocean basins. For example, Aniakchak CFE II tephra is present in both the Chukchi Sea and the North Atlantic Ocean (Jennings et al., 2011; Pearce et al., 2017). In addition, other eruptions with less precise age constraints are routinely dated using Bayesian models to integrate large volumes of differing chronological data (e.g.

Blockley et al., 2008; Keuhn et al., 2009; Davies et al., 2016). Combined with methodological advances in shard extraction (e.g. Turney et al., 1998; Blockley et al., 2005) and EPMA (e.g. Hayward, 2012), these techniques will no doubt continue to enhance the power of tephrochronology and provide new opportunities to use this technique in marine settings.

3.3.2 Methodological and taphonomic challenges

Previous studies have identified numerous tephra and cryptotephra deposits in ocean sediment cores from the North Atlantic as part of a tephra framework founded on Icelandic eruptions (e.g., Abbott et al., 2018b). These studies have described several methodological and taphonomic complications that must be considered in our interpretations of cryptotephra deposits from Placentia Bay and by future investigations of ultra-distal, North American cryptotephra deposits in ocean-sediments:

(i) Extracting sufficient shards for EPMA from low-concentration cryptotephra deposits is challenging, and the number of successful analyses is typically lower than shard counts. In ocean sediments, this is complicated by ~~dominate~~ dominant silt (63-2 μm) and clay (<2 μm) size fractions that can be difficult to remove with sieving, as well as abundant biogenic silica that includes densities similar to glass. In this study, we used large sample volumes (>3 cm^3) and a narrow range of densities (2.15 g/cm^3 and 2.45 g/cm^3) during heavy liquid separation for EPMA to mitigate these complications. While we achieved successful results with this method, cryptotephra deposits include a diverse range of volcanic glass (morphological and chemical composition), ~~and~~ so our approach may not be suitable in all settings. For example, heavy liquid densities of ≤2.45 g/cm^3 are unsuitable for extracting denser basaltic glass from host sediments.

(ii) Separating primary air fall events from reworked or ice-rafted detrital glass is a challenge in large parts of the North Atlantic that are affected (both directly and indirectly) by Icelandic volcanism (Abbott et al., 2018a). In this respect, settings such as Placentia Bay, which is sheltered from the strongest ocean currents and largely unaffected by ice rafting, may be more suitable for preserving discre~~e~~te tephra isochrons. The low shard concentrations in our study (<40 shards per gram) highlight the importance of site location and the sensitivity of ultra-distal cryptotephra deposits to background noise that could easily obscure the isochrons. A second example of identifying low-concentration cryptotephra deposits in the North Atlantic is provided by Jennings et al. (2014), who~~. They~~ report the presence of Aniakchak CFE II in an ocean core taken immediately east of Greenland. The coring site lies within the East Greenland Current that brings polar ~~, and importantly tephra free,~~ waters, which are less affected by ice-rafted tephra from Iceland, south – reaffirming the importance of site location and ocean conditions in successful studies.

(iii) Identifying the precise position of tephra isochrons in core AI07-10G is difficult as the peak in shard counts is not obvious in either deposit - both of which are composed of low shard concentrations without clear, discrete peaks above background noise. These complications are common in cryptotephra deposits (Lowe, 2011; Davies, 2015; references therein) in ocean sediments and can be exacerbated by bioturbation or sediment loading (Griggs et al., 2015). Because of these limitations, we suggest a conservative approach when using ocean cryptotephra deposits to synchronise palaeoenvironmental records (as we did) if isochrons are not clearly resolved in shard counts. Future studies, however, may identify better-

resolved isochrons, and there is potential to develop marine-terrestrial-cryosphere linkages using ultra-distal cryptotephra deposits.

4. Conclusions

Tephrochronology provides a means to establish local marine radiocarbon offsets. Understanding these offsets is essential in developing a robust chronology for ocean palaeoenvironmental records. In this study, we identify ~~the~~ Mazama Ash and White River Ash eastern lobe (WRAe) in Placentia Bay, North Atlantic Ocean. The precise ages of these isochrons and occurrence in depths close to radiocarbon dates allow us to refine the local marine radiocarbon reservoir to -126±151 years at ca. 7572±18 yr BP (the age of Mazama Ash) and -396±144 years at ca. ~~853~~1097±1 yr BP~~C.E.~~ (the age of WRAe). Changes in ΔR coincide with inferred shifts in water masses. The smaller absolute value of ΔR at the time of Mazama ash deposition occurs during a period, when the Slopewater Current is suggested to have strongly affected the Placentia Bay. The larger, more negative ΔR at the time WRAe deposition took place during a period when the inner Labrador Current was more influential (although still not dominant). By incorporating these chronological data within a Bayesian age-depth model with a variable radiocarbon offset (ΔR) we develop a chronology that better reflects uncertainties regarding marine carbon. Our findings demonstrate that reservoir ages may vary substantially within the Holocene. Therefore, it is critical to consider potentially variable ΔR when ocean circulation and ventilation characteristics have differed over time. Results from this study, and others in the North Atlantic, indicate that site location is an important factor in ~~the preservation of~~preserving marine cryptotephra isochrons, which are strongly impacted by taphonomy and ice rafting. Therefore, we suggest sheltered bays or areas influenced by currents that are unlikely to include re-worked volcanic ash are preferable.

Author contributions

AJM conceived the project. AJM, JH & BJ undertook cryptotephra analysis and interpretation. MSMB undertook Bayesian age modelling. MSS and CP provided chronology and materials. AJM wrote the manuscript with input from all the authors.

Acknowledgements

Are we are grateful to a Natural Sciences and Engineering Research Council of Canada Discovery Grant awarded to B. Jensen. We also acknowledge the Danish Council for Independent Research (grant no. 0135-00165B (GreenShelf) to MSS); the project has also received funding from the European Union's Horizon 2020 research and innovation program under Grant Agreement No. 869383 (ECOTIP) (MSS). Paul Zander and a second anonymous reviewer kindly took the time to provide constructive comments on an ealier draft of this manuscript.

Competing interests

Dr Britta Jensen is a member of the editorial board of Geochronology.

Code/data availability

All code/data used in this project is made available in Supplementary Information.

References

Abbott, P.M., Griggs, A.J., Bourne, A.J., and Davies, S.M.: Tracing marine cryptotephras in the North Atlantic during the last glacial period: Protocols for identification, characterisation and evaluating depositional controls. Marine Geology, 401, 81–97, doi:10.1016/j.margeo.2018.04.008, 2018a.

Abbott, P.M., Griggs, A.J., Bourne, A.J., Chapman, M.R., and Davies, S.M.: Tracing marine cryptotephras in the North Atlantic during the last glacial period: Improving the North Atlantic marine tephrostratigraphic framework. Quaternary Science Reviews, 189, 169–186, doi:10.1016/j.quascirev.2018.03.023, 2018b.

Alves, E.Q., Macario, K., Ascough, P., and Bronk Ramsey, C.: The worldwide marine radiocarbon reservoir effect: definitions, mechanisms, and prospects. Reviews of Geophysics, 56, 278–305, doi:10.1002/2017RG000588, 2018.

Ascough, P., Cook, G., and Dugmore, A.: Methodological approaches to determining the marine radiocarbon reservoir effect. Progress in Physical Geography, 29, 532–547, doi:10.1191/0309133305pp461r, 2005.

Blockley, S.P., Pyne–O'Donnell, S.D., Lowe, J.J., Matthews, I.P., Stone, A., Pollard, A.M., Turney, C.S., and Molyneux, E.G.: A new and less destructive laboratory procedure for the physical separation of distal glass tephra shards from sediments. Quaternary Science Reviews, 24, 1952–1960, doi: 10.1016/j.quascirev.2004.12.008, 2005.

Blockley, S.P., Ramsey, C.B., and Pyle, D.M.: Improved age modelling and high–precision age estimates of late Quaternary tephras, for accurate palaeoclimate reconstruction. Journal of Volcanology and Geothermal Research, 177, 251–262, doi:10.1016/j.jvolgeores.2007.10.015, 2008.

Borchardt, G.A., Aruscavage, P.J., and Millard, H.T.: Correlation of the Bishop Ash, a Pleistocene marker bed using instrumental neutron activation analysis. Journal of Sedimentary Petrology, 42, 301–306, doi:10.1306/74D72527-2B21-11D7-8648000102C1865D, 1972.

Bronk Ramsey, C. B.: Deposition models for chronological records. Quaternary Science Reviews, 27, 42–60, doi: 10.1016/j.quascirev.2007.01.019, 2008.

Bronk Ramsey, C. B.: Bayesian analysis of radiocarbon dates. Radiocarbon, 51, 337–360, doi: doi.org/10.1017/S0033822200033865, 2009a.

Bronk Ramsey, C. B.: Dealing with outliers and offsets in radiocarbon dating. Radiocarbon, 51, 1023–1045, doi:10.1017/S0033822200034093, 2009b.

Bronk Ramsey, C. B. and Lee, S.: Recent and planned developments of the program OxCal. Radiocarbon, 55, 720–730, doi: 10.1017/S0033822200057878, 2013.

Buckland, H.M., Cashman, K.V., Engwell, S.L., and Rust, A.C.: Sources of uncertainty in the Mazama isopachs and the implications for interpreting distal tephra deposits from large magnitude eruptions. Bulletin of Volcanology, 82, 1–17, doi: 10.1007/s00445-020-1362-1.

Bursik, M.I., Kobs, S.E., Burns, A., Braitseva, O.A., Bazanova, L.I., Melekestsev, I.V., Kurbatov, A., and Pieri, D.C.: Volcanic plumes and wind: Jetstream interaction examples and implications for air traffic. Journal of Volcanology and Geothermal Research, 186, 60–67, doi: 10.1016/j.jvolgeores.2009.01.021, 2009.

Bursik, M., Sieh, K., and Meltzner, A.: Deposits of the most recent eruption in the Southern Mono Craters, California: description, interpretation and implications for regional marker tephras. Journal of Volcanology and Geothermal Research 275, 114–131, doi:10.1016/j.jvolgeores.2014.02.015, 2014.

Catto, N.R., Hooper, R.G., Anderson, M.R., Scruton, D.A., Meade, J.D., Ollerhead, L.M.N., and Williams, U.P.: Biological and Geomorphological Classification of Placentia Bay: a Preliminary Assessment. Canadian Technical Report of Fisheries and Aquatic Sciences, 2289, 35, 1999.

Coulter, S.E., Pilcher, J.R., Plunkett, G., Baillie, M., Hall, V.A., Steffensen, J.P., Vinther, B.M., Clausen, H.B., and Johnsen, S.J.: Holocene tephras highlight complexity of volcanic signals in Greenland ice cores. Journal of Geophysical Research: Atmospheres, 117, doi:10.1029/2012JD017698.

Davies, L.J., Jensen, B.J., Froese, D.G., and Wallace, K.L.: Late Pleistocene and Holocene tephrostratigraphy of interior Alaska and Yukon: Key beds and chronologies over the past 30,000 years. Quaternary Science Reviews, 146, 28–53, doi: 10.1016/j.quascirev.2016.05.026, 2016.

Drinkwater, K.F.: Atmospheric and oceanic variability in the Northwest Atlantic during the 1980s and early 1990s. Journal of Northwest Atlantic Fishery Science, 18, 77–97, 1996.

Dyke, A.S.: An outline of North American deglaciation with emphasis on central and northern Canada. Developments in Quaternary sciences, 2, 373–424, doi:10.1016/S1571-0866(04)80209-4, 2004.

Egan, J., Staff, R., and Blackford, J.: A high–precision age estimate of the Holocene Plinian eruption of Mount Mazama, Oregon, USA. The Holocene, 25, 1054–1067, doi:10.1177/0959683615576230, 2015.

Eiríksson, J., Larsen, G., Knudsen, K.L., Heinemeier, J., and Símonarson, L.A.: Marine reservoir age variability and water mass distribution in the Iceland Sea. Quaternary Science Reviews, 23, 2247–2268, doi:10.1016/j.quascirev.2004.08.002, 2004.

Eiríksson, J., Knudsen, K.L., Larsen, G., Olsen, J., Heinemeier, J., Bartels–Jónsdóttir, H.B., Jiang, H., Ran, L., and Símonarson, L.A.: Coupling of palaeoceanographic shifts and changes in marine reservoir ages off North Iceland through the last millennium. Palaeogeography, Palaeoclimatology, Palaeoecology, 302, 95–108, doi:10.1016/j.palaeo.2010.06.002, 2011.

Gordon, J.E., and Harkness, D.D.: Magnitude and geographic variation of the radiocarbon content in Antarctic marine life: implications for reservoir corrections in radiocarbon dating. Quaternary Science Reviews, 11, 697–708, doi:10.1016/0277-3791(92)90078-M, 1992.

Filzmoser, P., Hron, K. and Reimann, C.: Principal component analysis for compositional data with outliers. Environmetrics: The Official Journal of the International Environmetrics Society, 621-632, https://doi.org/10.1002/env.966, 2009.

Griggs, A.J., Davies, S.M., Abbott, P.M., Coleman, M., Palmer, A.P., Rasmussen, T.L., and Johnston, R.: Visualizing tephra deposits and sedimentary processes in the marine environment: The potential of X-ray microtomography. Geochemistry, Geophysics, Geosystems, 16, 4329–4343, doi: 10.1002/2015GC006073, 2015.

Hayward, C.: High spatial resolution electron probe microanalysis of tephras and melt inclusions without beam–induced chemical modification. The Holocene, 22, 119–125, doi:10.1177/0959683611409777, 2012.

Heaton, T., Köhler, P., Butzin, M., Bard, E., Reimer, R., Austin, W., Bronk Ramsey, C., Grootes, P., Hughen, K., Kromer, B., Reimer, P., Adkins, J., Burke, A., Cook, M., Olsen, J., and Skinner, L.: Marine20 – the marine radiocarbon age calibration curve (0–55,000 cal BP). Radiocarbon, 62, 725–757, doi:10.1017/RDC.2020.68, 2020.

Heaton, T.J., Bard, E., Ramsey, C.B., Butzin, M., Hatté, C., Hughen, K.A., Köhler, P. and Reimer, P.J.: A response to community questions on the Marine20 radiocarbon age calibration curve: Marine reservoir ages and the calibration of 14C samples from the oceans. Radiocarbon, 1-27, DOI: https://doi.org/10.1017/RDC.2022.66, 2023.

Jennings, A., Thordarson, T., Zalzal, K., Stoner, J., Hayward, C., Geirsdóttir, Á., and Miller, G.: Holocene tephra from Iceland and Alaska in SE Greenland shelf sediments. Geological Society, London, Special Publications, 398, 157–193, doi:10.1144/SP398.6, 2014.

Jensen, B.J., Froese, D.G., Preece, S.J., Westgate, J.A., and Stachel, T.: An extensive middle to late Pleistocene tephrochronologic record from east–central Alaska. Quaternary Science Reviews, 27, 411–427, doi:10.1016/j.quascirev.2007.10.010, 2008.

Jensen, B. J., Pyne–O'Donnell, S., Plunkett, G., Froese, D. G., Hughes, P. D., Sigl, M., McConnell, J.R., Amesbury, M.J., Blackwell, P.G., van den Bogaard, C., Buck, C.E., Charman, D.J., Clague, J.J., Hall, V.A., Koch, J., Mackay, H., Mallon, G., McColl, L., and Pilcher, J. R.: Transatlantic distribution of the Alaskan White River Ash. Geology, 42, 875–878, doi: 10.1130/G35945.1, 2014.

Jensen, B.J., Beaudoin, A.B., Clynne, M.A., Harvey, J., and Vallance, J.W.: A re–examination of the three most prominent Holocene tephra deposits in western Canada: Bridge River, Mount St. Helens Yn and Mazama. Quaternary International 500, 83–95, doi:10.1016/j.quaint.2019.03.017, 2019.

Jensen, B.J., Davies, L.J., Nolan, C., Pyne–O'Donnell, S., Monteath, A.J., Ponomareva, V., Portnyagin, M., Booth, R., Bursik, M., Cook, E. and Plunkett, G.: A latest Pleistocene and Holocene composite tephrostratigraphic framework for northeastern North America. Quaternary Science Reviews, 272, 107242, doi:10.1016/j.quascirev.2021.107242, 2021.

Jessen, C.A., Solignac, S., Nørgaard-Pedersen, N., Mikkelsen, N., Kuijpers, A., and Seidenkrantz, M.S.: Exotic pollen as an indicator of variable atmospheric circulation over the Labrador Sea region during the mid to late Holocene. Journal of Quaternary Science, 26, 286–296, doi:10.1002/jqs.1453, 2011.

Knudsen, K.L. and Eirıksson, J.: Application of tephrochronology to the timing and correlation of palaeoceanographic events recorded in Holocene and Late Glacial shelf sediments off North Iceland. Marine Geology, 191, 165–188, doi: 10.1016/S0025-3227(02)00530-3, 2002.

Kuehn, S.C., Froese, D.G., Carrara, P.E., Foit, F.F., Pearce, N.J., and Rotheisler, P.: Major–and trace–element characterization, expanded distribution, and a new chronology for the latest Pleistocene Glacier Peak tephras in western North America. Quaternary Research, 71, 201–216, doi: 10.1016/j.yqres.2008.11.003, 2009.

Kuehn, S.C., Froese, D.G., and Shane, P.A.: The INTAV intercomparison of electron–beam microanalysis of glass by tephrochronology laboratories: results and recommendations. Quaternary International, 246, 19–47, doi: 10.1016/j.quaint.2011.08.022, 2011.

Lerbekmo, J.F.: The White river ash: largest Holocene Plinian tephra. Canadian Journal of Earth Sciences, 45, 693–700, doi:10.1139/E08-023, 2008.

Lowe, D.J.: Tephrochronology and its application: a review. Quaternary Geochronology, 6, 107–153, doi:10.1016/j.quageo.2010.08.003, 2011.

Lowe, D.J. and Hunt, J.B.: A summary of terminology used in tephra–related studies. Les Dossiers de l'Archaéo–Logis, 1, 17–22, 2001.

Mackay, H., Hughes, P.D., Jensen, B.J., Langdon, P.G., Pyne–O'Donnell, S.D., Plunkett, G., Froese, D.G., Coulter, S., and Gardner, J.E.: A mid to late Holocene cryptotephra framework from eastern North America. Quaternary Science Reviews, 132, 101–113, doi:10.1016/j.quascirev.2015.11.011, 2016.

Mackay, H., Plunkett, G., Jensen, B., Aubry, T., Corona, C., Kim, W.M., Toohey, M., Sigl, M., Stoffel, M., Anchukaitis, K., and Raible, C.: The 852/3 CE Mount Churchill eruption: examining the potential climatic and societal impacts and the timing of the Medieval Climate Anomaly in the North Atlantic Region. Climate of the Past Discussions, 18, 1475-1508, doi:10.5194/cp-18-1475-2022, 2022.

Mangerud, J.: The discovery of the Younger Dryas, and comments on the current meaning and usage of the term. Boreas, 50, 1–5, doi:10.1111/bor.12481, 2021.

McKay, N.P., Emile–Geay, J., and Khider, D.: geoChronR–an R package to model, analyze, and visualize age–uncertain data. Geochronology, 3, 149–169, doi:10.5194/gchron-3-149-2021, 2021.

Mello, L. and Rose, G.: Seasonal cycles in weight and condition in Atlantic cod (Gadus morhua L.) in relation to fisheries. Journal of Marine Science, 62, 1006–1015, doi:10.1016/j.icesjms.2005.03.008, 2005.

Monteath, A.J., Teuten, A.E., Hughes, P.D., and Wastegård, S.: Effects of the peat acid digestion protocol on geochemically and morphologically diverse tephra deposits. Journal of Quaternary Science, 34, 269–274, doi: 10.1002/jqs.3104, 2019.

Pearce, C., Seidenkrantz, M.–S., Kuijpers, A., Massé, G., Reynisson, N.F., and Kristiansen, S.M.: Ocean lead at the termination of the Younger Dryas cold spell. Nature Communications, 4, doi: 10.1038/ncomms2686, 2013.

Pearce, C., Seidenkrantz, M.S., Kuijpers, A., and Reynisson, N.F.: A multi–proxy reconstruction of oceanographic conditions around the Younger Dryas–Holocene transition in Placentia Bay, Newfoundland. Marine Micropaleontology, 112 39–49, doi:10.1016/j.marmicro.2014.08.004, 2014.

Pearce, C., Varhelyi, A., Wastegård, S., Muschitiello, F., Barrientos, N., O'Regan, M., Cronin, T.M., Gemery, L., Semiletov, I., Backman, J., and Jakobsson, M.: The 3.6 ka Aniakchak tephra in the Arctic Ocean: a constraint on the Holocene radiocarbon reservoir age in the Chukchi Sea. Climate of the Past, 13, 303–316, doi:10.5194/cp-13-303-2017, 2017.

Pilcher, J.R. and Hall, V.A.: Towards a tephrochronology for the Holocene of the north of Ireland. The Holocene, 2, 255–259, doi:10.1177/095968369200200307, 1992.

Plunkett, G. and Pilcher, J.R.: Defining the potential source region of volcanic ash in northwest Europe during the Mid–to Late Holocene. Earth–Science Reviews, 179, 20–37, doi:10.1016/j.earscirev.2018.02.006, 2018.

Pyne O'Donnell, S.D.F., Hughes, P.D.M., Froese, D.G., Jensen, B.J.L., Kuehn, S.C., Mallon, G., Amesbury, M.J., Charman, D.J., Daley, T.J., Loader, N.J., Mauquoy, D., Street–Perrott, F.A., and Woodman–Ralph, J.: High–precision ultra–distal Holocene tephrochronology in North America. Quaternary Science Reviews, 52, 6–11, doi: 10.1016/j.quascirev.2012.07.024, 2012.

Pyne–O'Donnell, S.D., Cwynar, L.C., Jensen, B.J., Vincent, J.H., Kuehn, S.C., Spear, R., and Froese, D.G.: West Coast volcanic ashes provide a new continental–scale Lateglacial isochron. Quaternary Science Reviews, 142, 16–25, doi: 10.1016/j.quascirev.2016.04.014, 2016.

Reimer, P.J. and Reimer, R.W.: A marine reservoir correction database and on–line interface. Radiocarbon, 43, 461–463, doi:10.1017/S0033822200038339, 2001.

Shaw, J., Piper, D.J.W., Fader, G.B.J., King, E.L., Todd, B.J., Bell, T., Batterson, M.J., and Liverman, D.G.E.: A conceptual model of the deglaciation of Atlantic Canada. Quaternary Science Reviews, 25, 2059–2081, doi:10.1016/j.quascirev.2006.03.002, 2006.

Shaw, J., Puig, P., and Han, G.: Megaflutes in a continental shelf setting, Placentia Bay, Newfoundland. Geomorphology 189, 12–25, doi:10.1016/j.geomorph.2013.01.010, 2013.

Sheldon, C.M., Seidenkrantz, M.S., Pearce, C., Kuijpers, A., Hansen, M.J., and Christensen, E.Z.: Holocene oceanographic changes in SW Labrador Sea, off Newfoundland. The Holocene, 26, 274–289, doi:10.1177/0959683615608690, 2016.

Sigl, M., Toohey, M., McConnell, J. R., Cole–Dai, J., and Severi, M.: Volcanic stratospheric sulfur injections and aerosol optical depth during the Holocene (past 11,500 years) from a bipolar ice core array. Earth System Science Data Discussions, 1–45, doi:10.5194/essd-14-3167-2022, 2022.

Sigl, M., Fudge, T. J., Winstrup, M., Cole–Dai, J., Ferris, D., McConnell, J. R., and Sowers, T. A.: The WAIS Divide deep ice core WD2014 chronology–Part 2: Annual–layer counting (0–31 ka BP). Climate of the Past, 12, 769–786, doi:10.5194/cp-12-769-2016, 2016.

Solignac, S., Seidenkrantz, M.S., Jessen, C., Kuijpers, A., Gunvald, A.K., and Olsen, J.: Late–Holocene sea–surface conditions offshore Newfoundland based on dinoflagellate cysts. The Holocene, 21, 539–552, doi:10.1177/0959683610385720, 2011.

Spano, N.G., Lane, C.S., Francis, S.W., and Johnson, T.C.: Discovery of Mount Mazama cryptotephra in Lake Superior (North America): implications and potential applications. Geology, 45, 1071–1074, 10.1130/G39394.1, 2017.

Thorarinsson, S.: Tephra studies and tephrochronology: a historical review with special reference to Iceland. In Tephra studies (pp. 1–12). Springer, Dordrecht, 1981.

Templ, M., Hron, K. and Filzmoser, P.: robCompositions: an R-package for robust statistical analysis of compositional data. Compositional data analysis: Theory and applications, 341-355, 2011.

Toohey, M. and Sigl, M.: Volcanic stratospheric sulfur injections and aerosol optical depth from 500 BCE to 1900 CE. Earth System Science Data, 809–831, doi: 10.5194/essd-9-809-2017, 2017.

Turney, C.S.M.: Extraction of rhyolitic component of Vedde microtephra from minerogenic lake sediments. Journal of Paleolimnology, 19, 199–206, doi: 10.1023/A:1007926322026, 1998.

Vale Inco., 2008. Environmental Impact Statement: Long Harbour Commercial Nickel Processing Plant. Vale Inco Newfoundland and Labrador Limited.

Vera, P.G.: Peter Filzmoser, Karel Hron, Matthias Templ: Applied compositional data analysis, with worked examples in R. Statistical Papers, 61, DOI:10.1007/s00362-020-01163-7, 921-922, 2020.

West, K.D. and Donaldson, J.A.: Evidence for winter eruption of the White River Ash (eastern lobe). Yukon Territory, Canada 29. May–2 June 2000, Geocanada 2000 – The Millennium Geoscience Summit, Conference CD, 2000.

Zdanowicz, C.M., Zielinski, G.A., and Germani, M.S.: Mount Mazama eruption: Calendrical age verified and atmospheric impact assessed. Geology, 27, 621–624, doi: 10.1130/0091-7613(1999)027<0621:MMECAV>2.3.CO;2 , 1999.

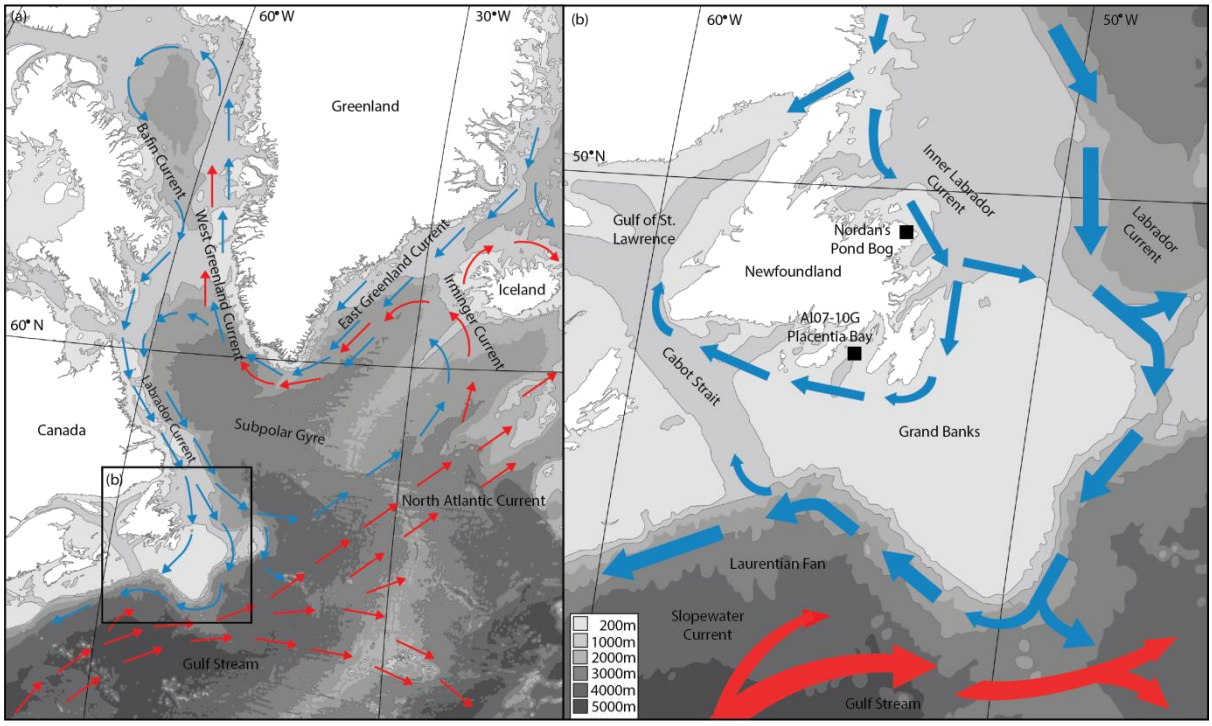

Figure 1: (a) Map showing the major surface/subsurface currents in the North Atlantic. (b) The surface and subsurface currents affecting Newfoundland and Placentia Bay. In both maps, blue arrows indicate cold, polar water, while red arrows indicate warmer, Atlantic-sourced water.

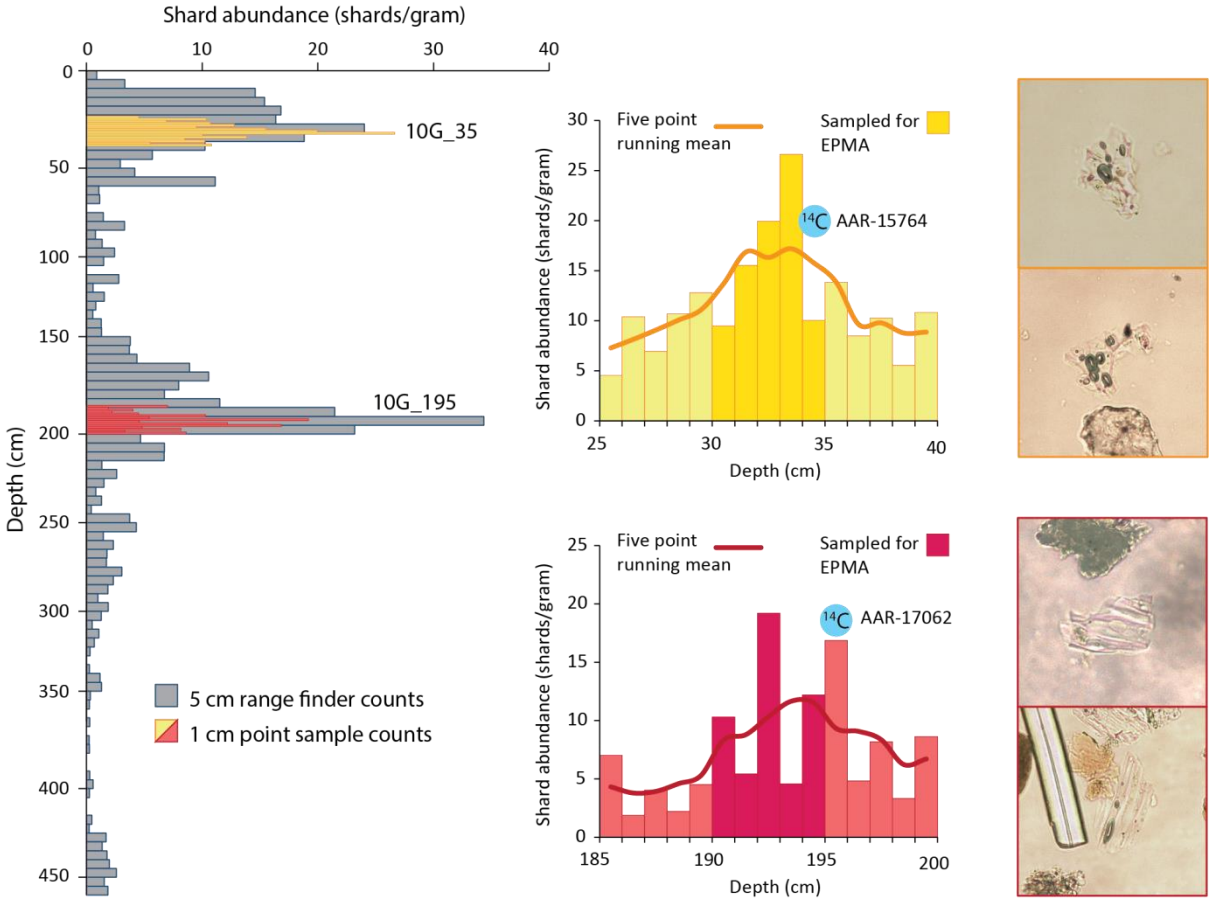

Figure 2: Shard counts and images from core AI07-10G, Placentia Bay, North Atlantic Ocean. Two shard peaks were found centred around core depths 32.5 cm (cryptotephra deposit 10G_35) and 192.5 cm (cryptotephra deposit 10G_195).

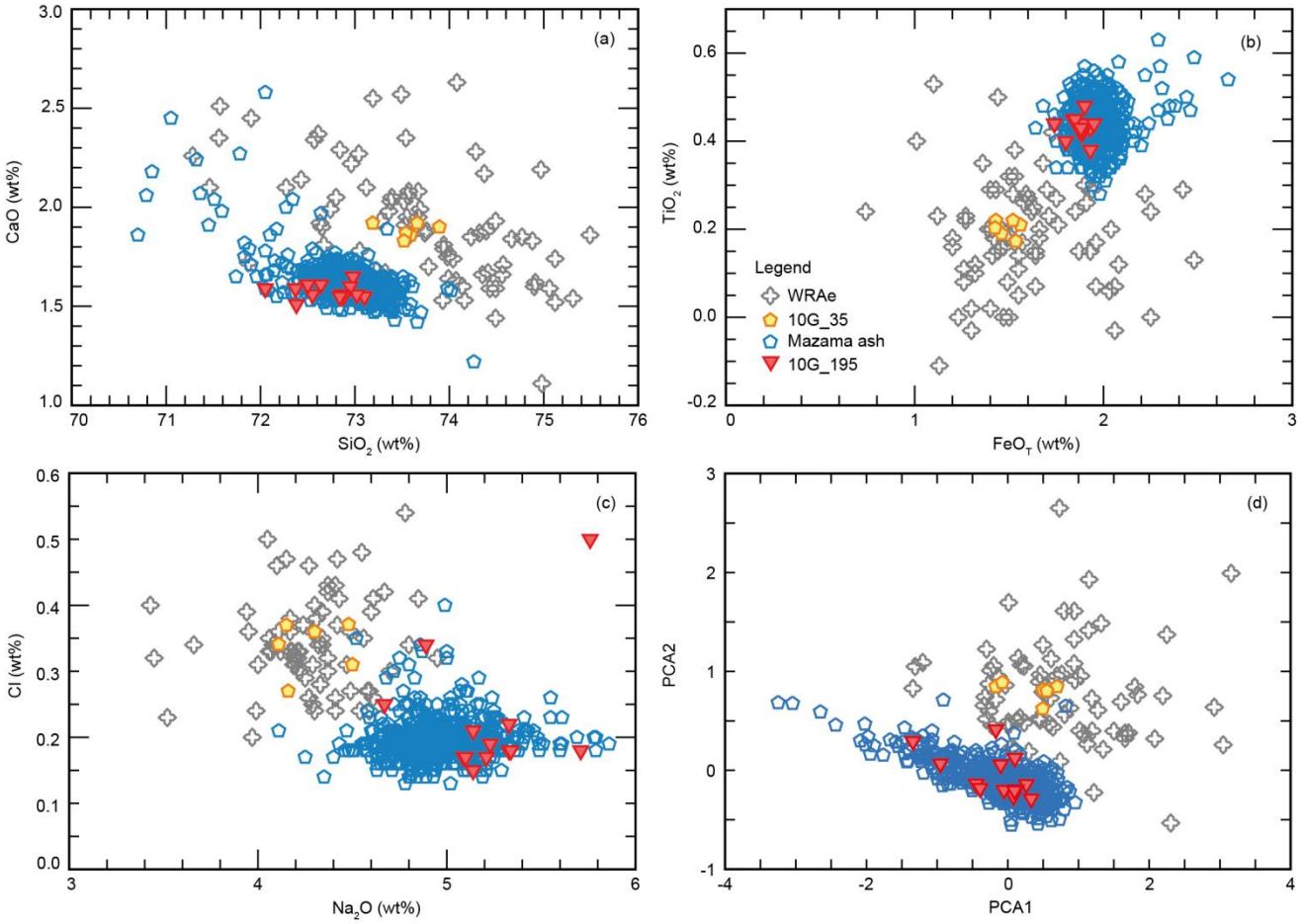

505

Figure 3: (a-c) Bi-plots of glass major-minor elements. (d) ~~Log-transformed~~Compositional Principle Component Analysis scores derived from glass major-minor elements. Comparative data includes EPMA analyses of Mazama Ash, excluding dacite shards which are rarely present in north-eastern North America (Jensen et al., 2019), and White River Ash eastern lobe (WRAe) (Jensen et al., 2014). Note that the three outlying 10G_195 analyses in panel c all have low analytical totals (<95%) (Table S1) and elevated Cl, which is likely to be derived from the epoxy resin mounting agent.

510

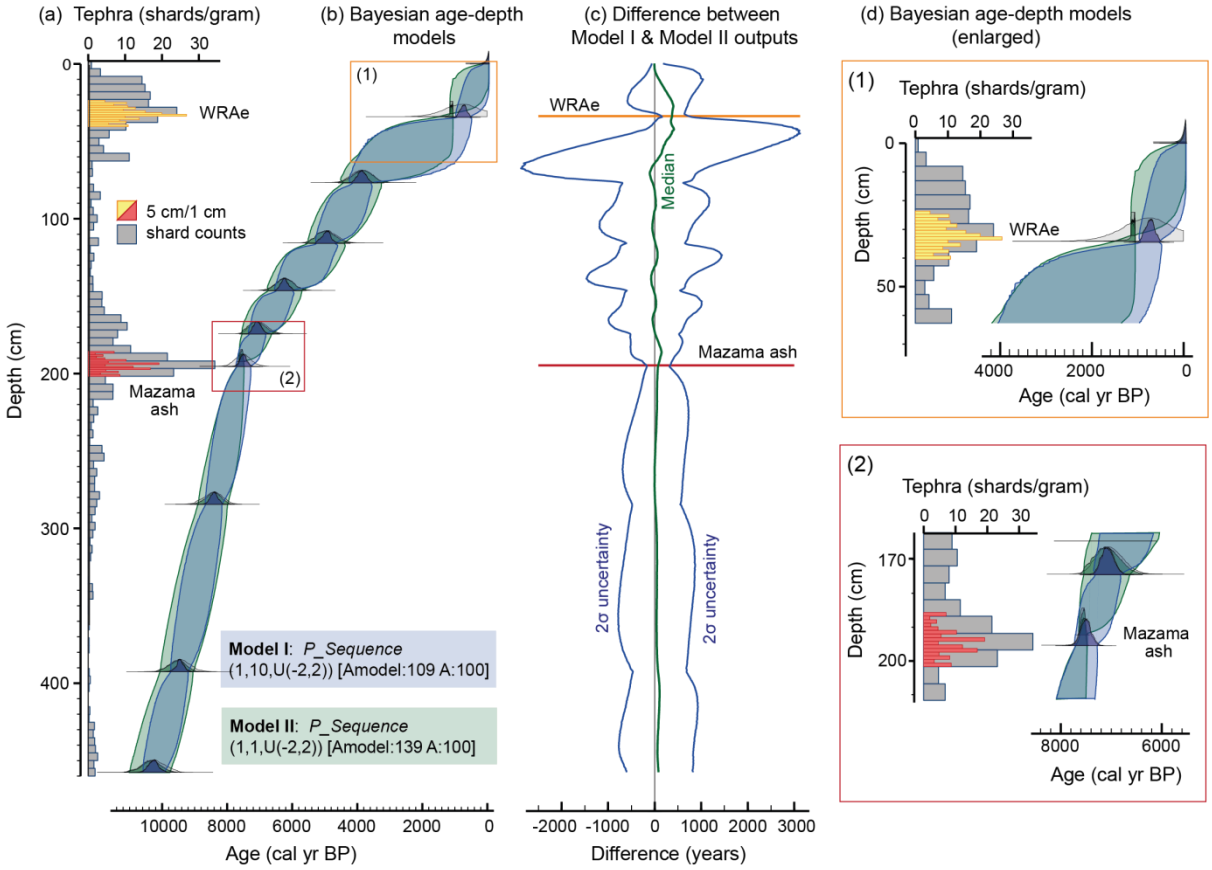

Figure 4: (a) Shard counts from core AI07-10G, Placentia Bay, North Atlantic Ocean. (b) Oxcal P_Sequence age-depth models. (c) The difference between Model I and Model II outputs. (d) Oxcal P_Sequence age-depth models zoomed in around the WRAe and Mazama Ash. All Oxcal models are shown at two sigma (95.4%) uncertainty. Light grey probability density functions show prior likelihoods; dark grey are posterior likelihoods.

Table 1: Radiocarbon (^{14}C) dates from core AI07-10G, Placentia Bay (Sheldon et al., 2016). Modelled age (I) refers to Bayesian age-depth model I and uses a single ΔR of -29±45 years. Modelled age (II) refers to Bayesian age-depth model II and uses a variable ΔR between -29±224 years. The ΔR is reported as mean and one standard deviations as this is routine for such data, making it easier to include in future age-depth modelling efforts.

Lab n.	Depth (cm)	Material	^{14}C age	Calibrated age (cal yr BP)	Modelled age (I) (cal yr BP)	Modelled age (II) cal yr BP)	ΔR (Model II)
AAR-15764	34-35	Mixed benthic foraminifera	1306±70	886-540	938-535	1491-1051	-451±151
AAR-17060	76.5-77.5	Mixed benthic foraminifera	3993±66	4060-3595	4145-3574	4420-3247	-10±213
AAR-15765	115.5-116.5	Mixed benthic foraminifera	4821±67	5177-4665	5259-4683	5525-4407	-50±210
AAR-17061	146-147	Mixed benthic foraminifera	5979±70	6399-5984	6483-5987	6738-5710	-25±221
AAR-15766	174-175	Mixed benthic foraminifera	6730±69	7246-6821	7318-6818	7552-6633	-50±210
AAR-17062	195-196	Mixed benthic foraminifera	7199±73	7669-7310	7709-7278	7706-7491	-91±106
AAR-15767	284-285	Gastropod (*Nuculana minuta*)	8072±73	8576-8171	8655-8160	8901-7994	-50±191
AAR-15768	392-393	Gastropod (*Nuculana minuta*)	8905±70	9600-9185	9736-9200	10086-9064	-103±201
AAR-12117	456-459	Mixed benthic foraminifera	9521±86	10495-9930	10583-9919	11027-9778	-101±209